DOI 10.1002/2015JC011096

Title: A reconciliation of empirical and mechanistic models of the air-sea gas transfer velocity

Contributing authors:

Lonneke Goddijn-Murphy (lead author)

ERI, University of the Highlands and Islands, Ormlie Road, Thurso, UK

David K. Woolf

ICIT, Heriot-Watt University, Stromness, UK

Adrian H. Callaghan

Scripps Institution of Oceanography, La Jolla, California, USA

Philip D. Nightingale

Plymouth Marine Laboratory, Prospect Place, Plymouth, UK

Jamie D. Shutler

University of Exeter, Centre for Geography, Environment and Society, Penryn, Cornwall, UK.

Corresponding author: Lonneke.Goddijn-Murphy@thurso.uhi.ac.uk

Key points:

1. The air-sea gas transfer model presented is consistent with data on a diverse set of gases
2. Bubble-mediated air-sea gas transfer cannot be ignored in strong winds
3. How the void fraction of bubble plumes could affect air-sea gas transfer velocity is discussed.

Index: 4504 (Air/sea interactions); 4599 (General or miscellaneous); 4820 (Gases)

Received: Jul 01, 2015; Revised: Dec 14, 2015; Accepted: Dec 18, 2015

Abstract

Models of the air-sea transfer velocity of gases may be either empirical or mechanistic. Extrapolations of empirical models to an unmeasured gas or to another water temperature can be erroneous if the basis of that extrapolation is flawed. This issue is readily demonstrated for the most well-known empirical gas transfer velocity models where the influence of bubble -mediated transfer, which can vary between gases, is not explicitly accounted for. Mechanistic models are hindered by an incomplete knowledge of the mechanisms of air-sea gas transfer. We describe a hybrid model that incorporates a simple mechanistic view – strictly enforcing a distinction between direct and bubble-mediated transfer – but also uses parameterizations based on data from eddy flux measurements of dimethyl sulphide (DMS) to calibrate the model together with dual tracer results to evaluate the model. This model underpins simple algorithms that can be easily applied within schemes to calculate local, regional or global air-sea fluxes of gases.

1. Introduction

1.1 Background

The gas fluxes between the atmosphere and the ocean (air-sea) are controlled by wind speed, sea state, sea surface temperature, near-surface turbulence and biological and chemical activity. Most regional and global flux estimates depend on a calculation using a standard bulk air-sea gas transfer formulation [e.g., *Takahashi et al.,* 2009]. For each gas, this calculation depends upon measurements of the gas concentration in both the surface ocean and the lower atmosphere, and upon the gas transfer velocity coefficient which describes the rate of transfer across the sea surface. Many gas flux and transfer velocity studies have focussed on carbon dioxide (CO_2) as this is a major greenhouse gas with large fluxes into and out of the ocean and plays an important role in ocean acidification. The fluxes of other atmospheric gases are also of fundamental importance to studies of marine productivity, biogeochemical cycles, atmospheric chemistry, Earth's climate, and human health [*Nightingale,* 2009]. In this paper we present a model for estimating gas transfer velocity for any chemically unreactive gas. The model is based on the knowledge that the air-sea exchange of the more poorly soluble gases is substantially enhanced by air-entraining wave breaking and specifically by bubble-mediated transfer. Our approach has similarities to that pursued by *Jeffery et al.* [2010] who used a modified version of the physically based NOAA-COARE (National Oceanic and Atmospheric Administration–Coupled-Ocean Atmospheric Response Experiment) model [*Jeffery et al.,* 2007]. In that model, the water-side transfer velocity is defined as a sum of direct gas transfer through the unbroken water surface and bubble-mediated gas transfer through the broken water surface via the *Woolf* [1997] parameterization. *Jeffery et al.* [2010] tune the modified NOAA-COARE model to a simple, empirical wind-speed-only parameterization. They show that for CO_2, the model is in agreement with a gas transfer velocity parameterization based on the global ocean inventory

of radiocarbon [*Sweeney et al.,* 2007] but predicts very different transfer velocities for other gases with substantially different solubilities to CO_2. In this current paper, rather than "tuning to Sweeney", we calibrate and evaluate the model using the most established parameterizations of field observations of gas transfer velocities. A general model should be consistent with data on all gases. We show that the popular quadratic and cubic models of gas transfer velocity to wind speed contradict the fairly linear relationship for dimethyl sulphide (DMS) and more soluble gases, and that a model that includes the solubility dependence of bubble-mediated transfer is more successful. We then show that this model can be expressed in the form of simple algorithms that can be readily applied to any gas at a local, regional or global scale. We note that in this paper we do not attempt a broad and balanced review of gas transfer across the air-sea interface, for this we refer the reader to *Garbe et al.* [2014]. We combine models of bubble-mediated gas transfer obtained from theory and laboratory experiments [*Woolf et al.*, 2007] with calibrations of gas transfer through the unbroken surface based on field measurements of DMS [*Goddijn-Murphy et al.*, 2012; 2013] and of field measurements of oceanic whitecapping [*Callaghan et al.*, 2008b]. This synthesis reveals new insights in the effect of the void fraction of the bubble plume of breaking waves on air-sea gas transfer of gases of different solubility. The consequences for the dual tracer method of air-sea gas transfer velocity (which is based on the extrapolation of gases of different solubility to the gas of interest) are shown.

1.2. Gas transfer velocity across the sea surface

The overall gas transfer velocity across the sea surface, K_w (m/s), appears as a key parameter in the standard bulk formula for air-sea gas transfer,

$$F = K_w\left(C_a/H - C_w\right) \qquad (1)$$

[*Liss and Merlivat,* 1986], where F (mol/(m^2 s)) is the gas flux (by our convention positive for a gas flux from the atmosphere to the ocean), C_a (mol/m^3) and C_w (mol/m^3) are the respective concentrations of the gas in the bulk air and bulk water, and H is the dimensionless gas-over-liquid form of the Henry's law constant (a function of temperature and salinity). The concentration difference is the thermodynamic driving potential and K_w the kinetic forcing function. K_w is dependent on the individual transfer velocities in water, k_w, and in air, k_a. It can be shown that for chemically unreactive gases,

$$1/K_w = 1/k_w + 1/(Hk_a) \quad (2)$$

[*Liss and Merlivat,* 1986]. For sparingly soluble gases the rate limiting step is transfer through the water-side. In this case, the term $1/k_w$ dominates equation (2), and k_w is often taken as a practical estimation of K_w. In this paper, we will concentrate our efforts on estimating the water-side transfer velocity, k_w, and use existing relations for k_a [e.g., *Goddijn-Murphy et al.,* 2012]. In section 3.4 we will explain how K_w can be calculated from k_w for any gas and under any set of conditions. We will express gas transfer velocities in commonly used unit of cm/h.

The water-side transfer velocity of a gas has a rather complicated dependence on the properties of the dissolved gas and upon environmental conditions, but a simple and practical parameterisation is often proposed based on the dominant role of wind-forcing and standard theories of turbulent transfer across a boundary. Most parameterisations conform to the general form:

$$k_w = \mathrm{Sc}^{-n}\left(a_0 + a_1 U + a_2 U^2 + a_3 U^3\right) \quad (3)$$

[*Wanninkhof et al.,* 2009] where [a_0, a_1, a_2, a_3] are coefficients (one or more of which may be set to zero) of a polynomial in wind-speed, U (at a standard elevation and corrected to neutral atmospheric stability), and Sc is the Schmidt number of the dissolved gas.

Following equation (3) above, it is apparent that transfer rates of different gases, or the same gas at a different water temperature, are often related through the Schmidt number

$$k_{w1}/k_{w2} = \left(\mathrm{Sc}_1/\mathrm{Sc}_2\right)^{-n} \tag{4}$$

where the exponent n is often taken to be 2/3 for smooth and immobile surfaces and 1/2 for rough or mobile surfaces [*Liss and Merlivat,* 1986; *Donelan and Wanninkhof,* 2002]. The Schmidt number is dependent on the specific gas, the water temperature, t, and to a lesser extent salinity, s. Sc can be calculated using equation (5)

$$\mathrm{Sc} = \nu_w / D_w = \eta_w / \left(\rho_w D_w\right) \tag{5}$$

where ν_w is the kinematic viscosity of water, D_w is the diffusivity of the dissolved gas of interest, and η_w and ρ_w are the dynamic viscosity and density of water respectively. *Johnson* [2010] shows how each of these terms can be calculated for a specific gas. Gas transfer velocities are typically normalized to a common Schmidt number to enable comparison between different gases. In this paper we will use a normalization of k_w to a Sc of 660 (the value for CO_2 in seawater at 20 °C) and a value for n of 1/2, thus $k_{w,660} = k_w\left(\mathrm{Sc}/660\right)^{1/2}$.

Many different relationships between transfer velocity and wind speed have been derived using different gases and methods giving a wide range of results (Figure 1). It should be noted that many of the relationships shown here are similar within the uncertainties associated with them. Also relationships are expanded beyond their range of measurement. However, they have been derived using a range of techniques. Most of these relationships

conform to the general form in equation (3), but *Liss and Merlivat* [1986] assume three linear segments of gas transfer with wind: the smooth regime, a regime with an undulating surface, and a regime with breaking waves. Most authors propose polynomial expressions of some kind, but with a limited number of non-zero coefficients. For example, *Wanninkhof* [1992] and *Ho et al.* [2006] both propose that only a_2 is non-zero ("a quadratic wind-speed dependence"), while *Wanninkhof and McGillis* [1999] propose that only a_3 is non-zero ("a cubic wind-speed dependence"). Estimated transfer velocities, local fluxes and the net fluxes in regions and globally depend on which coefficients are set to zero, and the value of the non-zero coefficients.

It is usually plausible to fit more than one polynomial expression to the same data [e.g., *Ho et al.,* 2007] and some judgement is required. A quadratic dependence of k_w on wind speed may appear reasonable given that the surface stress at the ocean surface also follows that dependence to a first approximation. However, it is not appropriate to directly compare a flux (wind stress is the air-sea flux of momentum) to a flux coefficient (a gas transfer velocity). Instead, flux coefficients can be compared if the bulk transfer formulae are written in a similar form [*Fairall et al.,* 2003; 2011]. If the wind stress is written as the product of a coefficient and the momentum difference, then it is apparent that the coefficient is in a first approximation linear in wind speed. Indeed, boundary layer theory suggests that all analogous coefficients including gas transfer velocities should be linear in wind speed. That principle appears to hold for turbulent heat transfer (sensible and latent) [*Fairall et al.,* 2011] and soluble gases ($K_w \approx k_a$) [*Yang et al.,* 2013] and the apparent non-linearity of k_w is peculiar. A successful model of air-sea gas transfer must be required to explain the empirical data and be consistent with theories of boundary layer transfer [*Wanninkhof et al.,* 2009].

One theory to explain the non-linearity of k_w is based on there being two significant pathways for transfer across the boundary layers on the water-side of the sea surface. Gas may be

transferred firstly by ordinary molecular and turbulent transfer, and secondly by bubble-mediated transfer where gas resides briefly within bubbles during the transfer process [*Woolf and Thorpe,* 1991]. These parallel pathways are then expressed as separate and additive contributions to the total kinetic rate. Thus, *Woolf* [1997] present a hybrid model in which k_w is a simple sum of the water-side gas transfer velocities through the unbroken sea surface, k_o, and through bubbles, k_b,

$$k_w = k_o + k_b \tag{6}$$

in which k_b alone is directly related to whitecap coverage, W. Another approach is an empirical model that relates W to turbulence effects on k_w and to bubble-mediated gas transfer [*Asher et al.*, 1996; 2002; *Asher and Wanninkhof*, 1998]. An approximately linear dependence on wind speed is proposed for k_o, consistent with theory [*Liss and Merlivat*, 1986], with DMS measurements [*Huebert et al.*, 2010; *Goddijn-Murphy et al.*, 2012; *Bell et al.*, 2015] and with the experience of the air-sea transfer of other quantities [*Fairall et al.,* 2003; 2011]. It is approximate because turbulence effects on k_0 are non-linear [*Asher et al.*, 1996; 2002; *Asher and Wanninkhof*, 1998] so using a more direct measurement of small scale sea surface roughness (than wind speed) would be preferable [*Goddijn-Murphy et al.*, 2012; 2013]. It is assumed that bubble-mediated transfer is approximately proportional to the cube of wind speed. That cubic dependence implies a relationship to the rate of wind energy input to the wave field, which makes sense since the injection of bubbles into the upper ocean should be proportional to the dissipation of wave energy. The simple description above is approximate and ignores processes related to buoyancy forcing (convection), surfactants, and variations in sea state development at a given wind speed. It also does not explicitly account for the bubble residence times below the water surface which is dependent on the initial

bubble plume injection depth, levels of background water turbulence, and larger scale circulation patterns such as Langmuir cells.

The Schmidt number relation equation (4) may be applicable to k_o with some caveats (the spatial and temporal uniformity of the thin film model equation (4) is based on is unrealistic, except perhaps in the calmest conditions [*Liss and Merlivat*, 1986]), but it is not credible for the term k_b [*Woolf,* 1993; *Asher et al.,* 1996; *Asher and Wanninkhof,* 1998]. The bubble-mediated transfer must be included for the least soluble gases in strong winds (> 10 m/s), but for relatively soluble gases, such as DMS, this term is expected to be negligible [*Woolf,* 1993; 1997]. The implication is that we should expect a fairly linear relationship of k_w to wind speed for DMS and more soluble gases (e.g. acetone or methanol) in direct contradiction to the popular quadratic and cubic models. Those quadratic and cubic models may be an adequate approximation for some gases, but a more complicated relationship may be obscured by experimental uncertainties. Also, we should not expect the same quadratic or cubic relationship to hold for all gases. *Jeffery et al.* [2010] found that both the transfer velocity of CO_2 and that of methane (CH_4) could be fitted adequately by general quadratic expressions (i.e. coefficients a_0, a_1 and a_2 are all non-zero) but the coefficients differ between the gases. *Yang et al.* [2014] concluded recently that for the oxygenated volatile organic compounds (OVOCs) methanol and acetone, water-side transfer velocities were consistent with a physical model based on distinct contributions of direct and bubble-mediated gas transfer. Estimates of k_w for these highly soluble gases are lower than k_w derived from sparingly soluble gases implying that tangential (shear driven) water-side transfer velocity dominates for soluble gases whereas for poorly soluble gases bubble-mediated transport is dominant at high wind speeds. *Woolf* [2005] constructed a hybrid model of the form of equation (6) by estimating k_o from wind-wave tank observations [*Jähne et al.,* 1987] and calculating k_b from an "independent bubble model" [*Woolf,* 1997]. In this paper, we follow a

similar approach but with new enhancements. We estimate k_o using a relationship retrieved in the field [*Goddijn-Murphy et al.*, 2012] and k_b from additional bubble models that take finite bubble plume void fraction into account [*Woolf et al.,* 2007].

2 Calibration of gas transfer through the unbroken sea surface

The simplest approach to estimating the direct transfer is to use data on a gas for which bubble-mediated transfer should be sufficiently weak to neglect. One suitable choice is DMS, though we do need to neglect a small contribution from bubble-mediated transfer (Fig. 6) and we must also correct for the slight effect of air-side resistance (i.e., $1/(Hk_a)$ in equation (2) is non-zero). *Goddijn-Murphy et al.* [2012] use DMS field measurements of K_w, t and s, and calculate H and k_a from t and s using the numerical scheme of *Johnson* [2010] to derive $k_{w,660}$ (equation (2)). This calculation implied that data $K_{w,660}$ was 2% to 13% smaller than $k_{w,660}$ for U_{10} ranging between 2.3 and 15.4 m/s and t between 5 and 30 °C [Fig. 6 in Goddijn-Murphy et al., 2012]. This effect of air-side resistance on air-sea gas transfer of DMS was considerably less than the correction predicted by *McGillis et al.* [2000] but not negligible. This approach is explained in more detail in two earlier papers [*Goddijn-Murphy et al.,* 2012; 2013] and the results are briefly summarised below.

Goddijn-Murphy et al. [2012] present calibrations of $K_{w,660}$ and $k_{w,660}$ of DMS as a function of *in situ* and satellite altimeter 10 m wind speed, U_{10}, and of Ku-band satellite altimeter backscattering coefficient, σ_{Ku}. For *in situ* wind speed ranging between 2 and 13.5 m/s the relation with $k_{w,660}$ expressed in cm/h is:

$$k_{o,660} \approx k_{w,660}(\mathrm{DMS}) = 2.6U_{10,is} - 5.7 \qquad (7)$$

[Table 4 in *Goddijn-Murphy et al.*, 2012]. The root-mean-square error of the fit is 4 cm/h. The U_{10} dependence is more gentle for altimeter wind speed $U_{10,al}$

($k_{w,660}(\mathrm{DMS}) = 2.2U_{10,al} - 3.4$), as was also recently found by *Bell et al.* [2015] ($k_{w,660}(\mathrm{DMS}) = 2.07U_{10,is} - 2.42$). These linear relations suggest that $k_{o,660}$ is less than zero for small wind speeds ($U_{10} < 2$ m/s) which is physically unrealistic because the sea surface is not necessarily perfectly smooth and also buoyancy (rather than stress) dominates gas exchange physics in near-zero wind. A more direct measurement of small scale sea surface roughness is the back-scattering coefficient, σ, through its inverse relation with wave slope. *Goddijn-Murphy et al.* [2012] found that for Ku-band satellite altimeter σ, $k_{w,660}(\mathrm{DMS}) = 2.1\times10^{3}\left(1/\sigma_{\mathrm{Ku}}\right)^{2} + 0.1$. This relationship implied that for smooth surfaces $k_{o,660}$ is 0.1 cm/h. Later *Goddijn-Murphy et al.* [2013] found evidence that using dual-band altimetry backscatter data (Ku-band and C-band) improved performance over previous single-band altimetry backscatter and wind speed parameterizations including the one using *in situ* data.

3 Gas transfer through the broken sea surface

3.1 Models of bubble-mediated gas transfer

The contribution of gas transfer through the broken surface depends on the solubility of the gas in seawater and therefore on sea surface temperature. Gas transfer is also highly sensitive to the void fraction (ratio of air volume to total volume) and bubble distribution of the bubble plume [*Woolf et al.,* 2007]. While *Jeffery et al.* [2010] only use the "independent bubble model" [*Woolf,* 1997], in this present paper we go one step further and also study the use of the "dense plume model" [*Woolf et al.,* 2007] that was derived from a combination of theory [*Woolf,* 1997] and laboratory experiments. We apply the calculations to derive water-side gas transfer velocity for CO_2 of Schmidt number 660 to compare our results with existing CO_2 parameterizations.

It is practical to estimate bubble-mediated gas transfer starting from a model of the number, size and depth distribution of bubbles entrained at the ocean surface and applying formula for their motion (their buoyant rise superposed on advection), compression and gas transfer across the surface of the bubbles. *Keeling* [1993] and *Woolf* [1993] independently made estimates of k_b based on the simple rise of a plume of bubbles after injection to a shallow depth. All of the models described below follow from the assumptions made by *Woolf* [1993], which have certain inherent implications. The time that each bubble is submerged was calculated based on each bubble rising freely at terminal velocity for only 0.1 m. Calculations were made for bubbles with both a free, mobile surface and an immobile surface, i.e. "clean" and "dirty" bubbles respectively, but only the results for a mobile surface were used in our predictions. The assumptions of a fixed and very low rise distance, the size distribution and the mobility of the surface are all open to question and discussed in section 3.2. *Woolf* [1997] found a non-linear fit of k_b as a function of the molecular diffusivity and the solubility of the gas in water at 20 °C. Building upon this work, *Woolf et al.* [2007] made a generalization of this non-linear fit to allow calculation of k_b at any water temperature and salinity (if the solubility and Schmidt number can be calculated). That model, "the independent bubble model" is summarised below. All of the models are scaled in terms of whitecap coverage. At whitecap coverage of 1%, the independent bubble model predicts for a shallow flux of clean bubbles:

$$k_{b,ind} = (Q_b/\alpha)(1+\chi^{1/f})^{-f}$$

$$\chi = Sc^{0.5}/(14\alpha) \qquad (8)$$

[*Woolf,* 1997], with Q_b the volume flux of bubbles of 24.5 (cm/h)/m^3, f (related to the breadth of the bubble plume distribution) of 1.2, and $\alpha(s, t)$ the Ostwald solubility of the gas (α is the

inverse of H). The value of Q_b was derived from the work of *Cipriano and Blanchard* [1981] who measured the size resolved bubble concentration beneath a continuous plunging water jet. Their bubble size distribution extended between lower and upper bubble radii of 0.025 mm and 4 mm respectively, and it exhibited a change in power law slope at about a radius of 1 mm that has since been shown to be characteristic of that found in breaking waves [e.g., *Deane and Stokes,* 2002], and which is described in more detail in section 3.3 below. *Woolf* [1997] calculated Q_b from the total volume flux of the simulated whitecap sized about 0.02 m^2 [*Cipriano and Blanchard*, 1981]. It is not certain that Q_b is the same for all oceanic whitecaps of the same size because penetration depth and rise speed of the bubbles can vary with environmental conditions, but it is difficult to quantify this uncertainty. The model is called the "independent bubble model" since one assumption is that the bubbles exchange gases with surrounding water independently of each other, where the dissolved gas content of that water is maintained at the mixed-layer average throughout. *Woolf et al.* [2007] point out that there should be a collective effect of the bubbles on the water surrounding them. In a very dense plume, we should expect the gas content of the interstitial water to change during the lifetime of that plume. If a finite volume of interstitial water is included then the "independent bubble model" can be modified to a "dense plume model" described by equation (9):

$$k_{b,void} = \left(XQ_b/\alpha\right)\left(1+\left(X\chi\right)^{1/f}\right)^{-f}$$

$$X = \alpha Q_p/\left(\alpha Q_p + Q_b\right) \qquad (9)$$

In the "dense plume model" Q_p is the volume flux of water within bubble plume relative to Q_b. With the void fraction, v, defined as $Q_b/(Q_b + Q_p)$ and $Q_b = 24.5$ it can be derived that $Q_p = 24.5/v - 24.5$. In this study we calculated $k_{b,mod,660}$ (cm/h) for W of 1% using both bubble

models for CO_2 at 20 °C and salinity of 35 (Table 3) and used *in situ W* data to estimate $k_{b,mod,660}$ in the field . The "independent bubble model" (equation (8)) gave $k_{b,ind,660}$ of 8.65 cm/(hW%), a little higher than *Woolf et al.* [2007] calculated for CO_2 at 20 °C in fresh water (8.5 cm/(hW%)). The results of the "dense plume model" (equation (9)) indicated that $k_{b,void,660}$ is lower than $k_{b,ind,660}$ and decreases with increasing void fraction (Figure 2). That result is the numerical manifestation of the "suffocation" of gas transfer described by *Woolf et al.* [2007]. Bubble-mediated gas transfer is always reduced by the collective effect and the reduction increases with void fraction.

3.2 Key assumptions of the model of bubble-mediated gas transfer explained

Equations (8) and (9) are based on the equilibration between the bubble and surrounding water, which is reasonable for weakly soluble gases such as CO_2. For a very poorly soluble gas with an equilibration time far greater than the time necessary to surface a "supersaturation term" should be added to account for the additional partial pressure on the gas in a submerged bubble [*Woolf and Thorpe,* 1991; *Woolf*, 1993; *Woolf*, 1997; *Woolf et al.*, 2007]. Supersaturation of the least soluble gases is increasingly important for smaller bubbles [*Woolf and Thorpe,* 1991].

Equations (8) and (9) are based on the behaviour of clean and mobile bubbles in a shallow plume. Surface organic material on dirty and immobile bubbles is likely to reduce k_b significantly due to lower molecular diffusion (lower individual bubble transfer velocities) and lower rise velocities (because gas transfer induced by the turbulence and flow around the bubble is reduced). For CO_2 at 20 ºC and dirty bubbles, *Woolf* [1993] estimated $k_{b,ind}$ of 2.63 cm/(hrW%). Most sources suggest that while natural systems are never truly clean, large bubbles generally behave as if they have mobile surfaces [*Woolf et al.*, 2007]. We assume that bubble-mediated gas transfer is mainly through larger bubbles, which is supported by the experiments of *Deane and Stokes* [2002] that show that the initial volume of air entrained by

a breaking wave is dominated by bubbles with radii around and above 1 mm (section 3.3). Because smaller bubbles rise slower, and attract more dirt as they rise to the surface, the assumption of a clean surface is less convincing.

It is difficult to be exact, but Table 1 shows estimates of the consequences of the key assumptions made. It shows that for a very poorly soluble gas the effects are bigger than for a reasonably soluble gas and that the assumption of a clean/mobile bubble surface has the most significance. For 1% whitecap coverage and dirty bubbles $k_{b,ind}$ is estimated to be 6 to 10 cm/h lower for reasonably soluble and very poorly soluble gas respectively. If we approximate the resulting uncertainties in $k_{b,ind}$ of ±3 to ±5 cm/h, the total known uncertainty in k_w due to uncertainty in the mobility of the bubble surfaces would be ±5 to ±7 cm/(hW%), and higher if we consider the other assumptions. For a detailed comparison of applications of equations (8) and (9) to clean bubbles, dirty bubbles (using the original equations in [*Woolf*, 1993]) and a mix of small dirty bubbles and large clean bubbles we refer the reader to [*Woolf et al.*, 2007].

3.3 Whitecap measurements and void fraction

For the application of both the "independent bubble model" and the "dense plume model" of bubble-mediated gas transfer, values of fractional whitecap coverage, W, are required; for the "dense plume model" the void fraction of the bubble plume is needed as well. Given the difficulties of measuring bubble plume size distributions, void fractions, and bubble plume injection depths in breaking waves at sea, fractional whitecap coverage is often used as a pragmatic tool to scale bubble-mediated processes to open ocean conditions [e.g., *Monahan et al.,* 1983; *Woolf,* 2005; *Callaghan,* 2013].

The W values used here were derived from images of the sea surface taken at 0.5 Hz within 30 minute periods, and calculated as the percentage of pixels with intensity value above a

threshold value obtained using Automated Whitecap Extraction (AWE). These *W* data were generated as part of the Marine Aerosol Production (MAP) campaign, and are described in detail in [*Callaghan et al.,* 2008b]. The image processing algorithm automatically determines the optimal threshold intensity for whitecap detection for every individual image. For each *W* data point the *W* values of hundreds of images were averaged, a sufficient number to achieve convergent values [*Callaghan et al.,* 2008a; *Callaghan and White,* 2009].

The MAP *W* data represent contributions from all stages of whitecap foam evolution. The foam signal that marks areas of actively breaking waves is often termed Stage A, while the decaying foam area is commonly termed Stage B [*Monahan and Lu*, 1990]. Their sum refers to total whitecap coverage, *W*. Here we have assumed that bubble-mediated gas exchange is proportional to total fractional whitecap coverage, which is essentially used as a proxy for the volume flux of air due to wave breaking. However, as explained in the following, in certain situations this may not be entirely valid. For example, the persistence time of individual whitecaps is dependent on the flux of bubbles to the surface and also on surface active materials (surfactants) in the water column that can act to stabilize bubbles and foam cells against rupture [*Monahan,* 1971; *Monahan and Lu,* 1990; *Sharkov,* 2007; *Callaghan et al.,* 2012; 2013]. Bubble plume injection depth and water chemistry are therefore important factors determining the lifetime of individual whitecaps, and hence values of *W*. For a given flux of bubbles to the water surface, *W* is expected to be greater when water chemistry plays a significant role stabilizing bubbles and foam cells against rupture. In this case, whitecap-scaled oceanic bubble-mediated gas exchange may be over-estimated because of this surfactant effect. In terms of the stages of the whitecap evolution, it is often assumed that only W_A contributes to air-sea gas exchange. This has not been conclusively shown, and would only be true if the trace gas in the bubble plume completely equilibrated with the surrounding water during active breaking, with no exchange occurring as the bubbles rise

back to the surface sustaining the decaying whitecap signal (W_B). While oceanic field data show substantial variation in individual whitecap lifetimes (largely driven by variations in whitecap decay time) it is not yet known to what extent natural oceanic surfactants influence values of W on various spatial and temporal scales. Until the relative contribution of the natural oceanic surfactant effect is evaluated and can be effectively removed from W_B or W, total whitecap coverage remains a practical but imperfect scaling term for bubble-mediated processes.

The void fraction associated with actively breaking crests and decaying foam patches is an important parameter in predicting bubble-mediated gas transfer. It clearly affects bubble-mediated gas transfer (Figure 2) but it is difficult to measure in the field, and harder to predict. Indeed, according to *Woolf et al.* [2007], larger values of void fraction do not necessarily lead to larger gas fluxes due to what is termed the suffocation effect. In-situ instruments such as optical fibre-probes and conductivity probes can detect the phase (air and water) of the flow at a given location and instance in time, and such measurements can be averaged in time and space to provide estimates of void fraction within these turbulent two-phase flows [e.g., *Lamarre and Melville,* 1991; *Blenkinsopp and Chaplin,* 2007; *Hoque and Aoki,* 2014; *Lim et al.,* 2015]. Alternatively, measured bubble size distributions can be integrated over a range of bubble radii following

$$v = \frac{4}{3}\frac{\pi}{V}\int_{a_{\min}}^{a_{\max}} n(a)a^3 da \qquad (10)$$

where a is the bubble radius and $n(a)$ is the number of bubbles per unit volume of the two-phase air-water flow per unit increment bubble radius, da, and V is the volume of the two-phase air-water flow [e.g., *Deane and Stokes,* 2002; *Leifer and Leeuw,* 2006]. Figure 3a shows a canonical bubble size-distribution for a laboratory breaking wave reported in *Deane and Stokes* [2002]. The distributions of large $(a >\sim 1\ mm)$ and small bubbles $(a <\sim 1\ mm)$

are described by power laws $n(a) = \beta_2 a^{-10/3}$ and $n(a) = \beta_1 a^{-3/2}$, respectively. The point of intersection occurs at a bubble radius termed the Hinze scale which represents the largest bubble that is stabilized against turbulent fragmentation within the breaking wave [*Deane and Stokes,* 2002]. Scaling the bubble size distribution by bubble volume shows that even though smaller bubbles are most numerous, it is the population of bubbles at the Hinze scale that contributes most significantly to the air volume within the initial bubble plume. Figure 3b shows the probability distribution of air volume as a function of bubble size for the bubble size distribution in figure 3a. It reveals the importance of measuring supra-millimetre bubbles when accurately characterizing the initial volume of air entrained by a breaking wave.

Despite its importance, relatively little is known about values of void fraction within the water column beneath oceanic whitecaps due to the difficulty of making such measurements. *Bowyer* [2001] reports maximum values between 0.1-0.2 at depths of about 10 cm, derived from measurements of $n(a)$. *Deane and Stokes* [2002] report maximum void fractions of 0.065 at 30 cm depth beneath oceanic whitecaps about 1 s into the quiescent phase of plume degassing when active air entrainment has ceased, and *Stokes et al.* [2002] report peak void fractions of order 0.1 during whitecap events also measured at 30 cm depth. These three studies all highlight the importance of making bubble measurements that are close in time and space to actively breaking waves. *De Leeuw and Cohen* [2002] also report oceanic bubble size distributions, but the largest bubble measured had a radius of about 0.5 mm indicating these measurements likely did not capture the peak in the bubble size distribution (see Figure 3).

Many more laboratory studies have yielded a great deal of information on void fractions and bubble size distributions within breaking waves. Extensive measurements by *Lim et al.*

[2015] highlight the large degree of spatial and temporal heterogeneity in v in laboratory plunging breakers. Depth-resolved measurements of v averaged over the period of the breaking wave show peak void fraction values of between 0.05 and 0.2 within 5-10 cm of the water surface, which decrease quasi-linearly below this. Time-resolved depth averages of void fraction show a quasi-linear increase with time that peaked between 0.1 and 0.4 at different spatial points within the breaking wave (e.g., the cavity collapse and splash-up regions), which was then followed by a quasi-exponential decay with time, and peak void fractions were associated with the cavity collapse region of the breaking wave. Depth-averaged levels of void fraction above 0.01 persisted for less than about 0.5 s to 1 s. It is worth noting here that the models of bubble-mediated gas transfer (section 3.1) are based on shallow and short-lived bubbles and therefore it is the size distribution and void fraction very close to a breaking that are most pertinent.

While much work has been done to characterize void fraction within laboratory breaking waves, there is a dearth of measurements in the open ocean, especially with concurrent measurements of W. However, the limited ocean data, along with the laboratory results, indicate that void fraction can be expected to be spatially and temporally heterogeneous during wave breaking and subsequent bubble plume degassing. We refer the reader to *Kiger and Duncan* [2012], *Anguelova and Huq* [2012], and *Lim et al.* [2015] for further information on void fraction within breaking waves.

3.4 A hybrid model of gas transfer velocity

We can estimate K_w and k_w for any gas and under any set of conditions (s,t,v) by using the equations presented in the previous sections. First we derive water-side gas transfer velocity, k_w, which is a simple sum of direct and bubble-mediated gas transfer, k_o and k_b respectively (equation (6)). For estimating k_o we use the $k_{w,660}$ parameterization for DMS (e.g., equation (7)) and apply the Schmidt number dependence (equation (4)):

$$k_{\mathrm{o}}(\mathrm{gas},s,t) = k_{\mathrm{o},660}\left(\mathrm{Sc}(\mathrm{gas},s,t)/660\right)^{-1/2} \quad (11)$$

In place of equation (7) another k_o estimation could be used, for example $k_{w,660}$(DMS) as a function of satellite altimeter U_{10} or backscattering coefficient [*Goddijn-Murphy et al.,* 2012; 2013]. The bubble-mediated gas transfer, k_b, can be approximated with either the "independent bubble model" (equation (8)), or, if the void fraction of the bubble plume is accounted for, the "dense plume model" (equation (9)):

$$k_{\mathrm{b}}(\mathrm{gas},s,t,v) = k_{\mathrm{b,mod}}\left(s,t,v,\mathrm{Sc}(\mathrm{gas},s,t),\alpha(\mathrm{gas},s,t)\right)\times W\% \quad (12)$$

with $k_{b,mod}$ indiciating $k_{b,ind}$ or $k_{,b,void}$ respectively. In equation (12) whitecap fraction W is either measured or parameterized, and information about how to compute Sc and α for a range of gases in seawater is known [*Johnson,* 2010; *Wanninkhof,* 2014]. Overall gas transfer rate K_w can then be calculated using equation (2), with $H = 1/\alpha$:

$$K_{\mathrm{w}}(\mathrm{gas},s,t,v) = \left(1/k_{\mathrm{w}}(\mathrm{gas},s,t,v) + \alpha(\mathrm{gas},s,t)/k_{\mathrm{a}}(U_{10},\mathrm{Sc}_{\mathrm{a}}(\mathrm{gas},t_{\mathrm{air}})\right)^{-1} \quad (13)$$

In equation (13) k_w(gas,s,t,v) is the sum of k_o(gas,s,t) and k_b(gas,s,t,v) (equation (6)) with k_o(gas,s,t) and k_b(gas,s,t,v) from equations (11) and (12) respectively. Air-side gas transfer velocity, k_a, is mainly a function of wind speed, temperature, t_{air}, and Schmidt number, Sc_a, in air; Sc_a and k_a can be calculated using a numerical scheme [*Johnson,* 2010]. For CO_2 the term k_a is usually ignored but for more soluble gases such as DMS k_a should be accounted for. An overview of the different k definitions and how they can be estimated for an insoluble-, soluble- or any gas is given in Table 1 in *Goddijn-Murphy et al.* [2012].

3.5 Implications of bubble-mediated gas transfer for the dual tracer method

Having used a relatively soluble gas to estimate the direct transfer velocity, we needed data on less soluble gases to establish the bubble-mediated contribution. A variety of data are

applicable, but among the most important data is that from dual tracer (DT) experiments [e.g., *Nightingale et al.,* 2000; *Ho et al.,* 2006]. It must be noted however that the dual tracer method (as usually presented) relies entirely on an assumption that gas transfer velocity is proportional to $Sc^{-1/2}$ (equation (4)). That assumption was validated by *Watson et al.* [1991] using lake data and by *Nightingale et al.* [2000] using a third non-volatile tracer. The assumption is also clearly consistent with any model of the form of equation (3) with $n = 1/2$ and therefore dual tracer data can be used to calibrate or validate a number of models without hesitation. For our model, however, a little more thought is needed. The assumption is entirely consistent with our model for direct transfer and thus if bubble-mediated transfer is negligible there need be no significant reinterpretation of dual tracer data. However, if and where the bubble-mediated transfer provides a significant contribution to the totals, some reinterpretation of dual tracer is necessary.

We investigated the consistency of published dual tracer data with our models, firstly by considering the published results compared to the predicted direct transfer (equation (7)). Can the published values of k_w be readily explained by the expected direct transfer? According to equation (7), the direct transfer should be about 20 cm/h at wind speeds of around 10 m/s (normalized to a Schmidt number of 660; this translates to about 21cm/h for a Schmidt number of 600). In fact, numerous dual tracer results for moderate-to-strong winds cluster around these values [e.g., *Nightingale,* 2009] implying both that bubble-mediated transfer might be negligible at these wind speeds and that an assumption that transfer velocity is proportional to $Sc^{-1/2}$ is supportable (this is also consistent with the previous validation using a third tracer at a similar wind speed [*Nightingale et al.,* 2000]). Relatively few dual tracer results have been reported for stronger winds, but these have heavily influenced the general view on the behaviour of gas transfer velocities in strong winds [e.g., *Nightingale,* 2009]. These few values suggest transfer velocities in excess of 50 cm/h at a wind speed of 15 m/s,

while our model only predicts direct transfer of 35 cm/h at most. Therefore, there is a case for looking further at the dual tracer results and asking how those results might be affected by bubble-mediated transfer.

We have compared the transfer velocities inferred using the standard dual tracer method, with transfer velocities predicted by our models, as follows. In the standard dual tracer method K_w is measured and because insoluble gases are used K_w is an estimation of k_w (equation (2)). The difference between k_w of two tracer gases, $\Delta k_w = k_{w,1} - k_{w,2}$, gives k_w of either one of the tracer gases of a different Schmidt number or a third gas (under the assumption of equation (4)):

$$k_{w,3} = \left(k_{w,1} - k_{w,2}\right)\mathrm{Sc}_3^{-n}\mathrm{Sc}_1^{n}\mathrm{Sc}_2^{n} / \left(\mathrm{Sc}_2^{n} - \mathrm{Sc}_1^{n}\right) \qquad (14)$$

[*Watson et al.,* 1991]. *Watson et al.* [1991] calculated k_w for CO_2 at 20 °C under stormy conditions from measurements of the tracer gases ^{3}He and SF_6 by assuming $n = 1/2$. Both tracer gases are less soluble than CO_2. Nightingale *et al.* [2000] corrected the shipboard U_{10} in the *Watson et al.* [1991] data which increased the dependence of $k_{w,600}$ on U_{10} significantly, particularly for high wind speeds. *Woolf* [1993] notes that it is worth considering that if a significant fraction of k_w of the tracers is mediated through bubbles this could affect Δk_w and the inference of k_w of a more soluble gas. We used equations (6) and (14) to estimate the propagation of the different contributions of bubble-mediated gas transfer of the tracer gases in DT-measured $k_{w,660}$. This quantity, $k_{b,660}^{DT}$, for a W of 1%, can be calculated with

$$k_{b,660}^{\mathrm{DT}} = \Delta k_b \left(\mathrm{Sc}_{^3\mathrm{He}}/660\right)^{0.5} / \left(1 - \left(\mathrm{Sc}_{^3\mathrm{He}}/\mathrm{Sc}_{\mathrm{SF}_6}\right)^{0.5}\right) \qquad (15)$$

with $\Delta k_b = k_{b,3He} - k_{b,SF6}$. The terms $k_{b,3He}$, and $k_{b,SF6}$ were calculated with the "independent bubble model" (equation (8)) and the "dense plume model" for different void fractions (equation (9)). Those "dual-tracer values", $k_{b,mod,660}^{\mathrm{DT}}$, can be compared to $k_{b,mod,660}$ calculated

directly from the model equations (8) and (9). The Ostwald solubility and Schmidt number for the different gases were calculated as a function of temperature and for salinity of 35 [*Wanninkhof,* 1992]. If $k^{DT}_{b,mod,660}$ is greater (smaller) than $k_{b,mod,660}$ then the DT method would overestimate (underestimate) the transfer velocity of CO_2. The differences between $k^{DT}_{b,mod,660}$ and $k_{b,mod,660}$, plotted in Figure 4, show that according to the "independent bubble model" and the "dense plume model" for low void fractions DT overestimates $k_{b,660}$ (and hence $k_{w,660}$) while for higher void fractions DT underestimates. In addition to void fraction, the differences are also dependent on temperature. Figure 4 indicates that according to the "independent bubble plume" model and for t of 20 °C the dual tracer method would overestimate k_b by over 4 cm/h per 1% W. According to the "dense plume model", this difference would be 2 cm/h and -2 cm/h for respective v of 0.1 and 0.5 and near zero for a v of ~0.25. In general, it appears that the dual tracer method should give a useful prediction of the transfer velocity of CO_2; however there is a significant but uncertain bias (positive for independent bubbles and low void fractions and negative for high void fractions) in strong winds.

4. Evaluation of the Hybrid Model

For the evaluation of the hybrid model for a relatively insoluble gas it was most convenient to consider k_w of CO_2 gas in seawater at t of 20° (Sc of 660) but it could be for any other gas or set of conditions (section 3.4). The bubble-mediated gas transfer models are for a value of W of 1%, so to fully understand bubble-mediated gas transfer we need an expanded set of W values. *Woolf* [2005] and *Fangohr and Woolf* [2007] use a relation for k_o retrieved in a wind wave tank and a sea state dependent parameterization of W in their application of the hybrid model (equation (6) and "independent bubble plume"). However, there are large differences in existing W parameterizations and the scatter within the various datasets is great [e.g.,

Anguelova and Webster, 2006; *de Leeuw et al.,* 2011]. We therefore used *in situ* U_{10} and W data to test the hybrid model. We used data from *Callaghan et al.* [2008b] because it includes high U_{10} values, up to 23.1 m/s, and consequently high W data, between 0.002% and 7.5% (2% on average). In addition these W data are of high quality and have been previously used in a study of parameterizations and algorithms for oceanic whitecap coverage [*Goddijn-Murphy et al.,* 2011]. These W data were collected under sea surface temperatures of between 12.99 °C – 13.77 °C, but as a recent laboratory study suggests that the temperature dependence of W is only of order 10 - 30% for temperatures between 5 °C of and 30 °C [*Callaghan et al.,* 2014] we assumed W was the same as for 20 °C. With k_w the sum k_o approximated by k_w of DMS (equation (7)) and k_b estimated by the product of modelled k_b and *in situ* W% we used

$$k_{w,660} = 2.6U_{10,is} - 5.7 + k_{b,mod,660}W\% \quad (16)$$

In equation (16) subscript "mod" indicates "ind" or "void" for respective "independent bubble model" (equation (8)) or "dense plume model" (equation (9)). The results of applying the hybrid parameterization to the W and U_{10} data from *Callaghan et al.* [2008b] data are plotted in Figure 5a. The hybrid model predictions with the "independent bubble model", $k_{w,660,ind}$, are closest to N00 [*Nightingale et al.,* 2000] followed by H06 [*Ho et al.,* 2006] with a slightly steeper curve for H06. The values calculated with the "dense plume model", $k_{w,660,void}$, are lower and decreasingly lower with increasing void fraction and wind speed (not shown). In Figure 5b $k_{w,660,ind}$ is shown together with $k_{w,660,void}$ using a v of 0.5 to illustrate how the void fraction can theoretically affect gas transfer velocity. A v of 0.5 would be exceptional and should indicate the maximum expected impact of the void fraction. An ANOVA applied to the $k_{w,660,ind}$ and $k_{w,660,void}$ data returned a p-value of 0.17, implying that

using the MAP whitecap coverage observations the $k_{w,660,ind}$ and $k_{w,660,void}$ difference was not very significant.

5. Discussion

We have described a fairly simple semi-empirical model of gas transfer velocity with a linear dependence of direct transfer on (neutral stability) wind speed. This simple model can be easily applied to *in situ* or satellite observed U_{10} data. A more physically complete description is given by the NOAA-COARE model [*Fairall et al.,* 2011]. However, the empirical evidence for the characteristics of direct transfer is quite limited.

The qualitative description of bubble-mediated transfer is also uncertain. In comparing the result of the original "independent bubble model" [*Woolf,* 1997] to dual tracer results, we find an adequate validation and there does not seem to be a strong case for replacing this model. The uncertainty in the bubble-mediated transfer is partly expressed by the "dense plume model" and how the void fraction could have some effect on bubble-mediated gas transfer (Figure 2). A comparison between Figures 5a and 5b implies that the wide range of previous k_w parameterizations (Figure 1) could not be explained by different void fraction conditions between the surveys on which the parameterizations were based. However, void fractions changing during a survey could explain part of the scatter in scatter plots of U_{10}-k [e.g., Figure 2 in *Ho et al.,* 2006]. (A lot of the data scatter in these plots could be related to the poor representation of W by U_{10} only since many sea states can be present at a given U_{10} [*Woolf,* 2005].) It is difficult to decide which value for void fraction to use and additional knowledge about bubble plume distributions, developments and void fractions (evolving over the lifetime of individual whitecaps) in the ocean is needed to develop the hybrid model. The discussion of field and laboratory measurements of void fraction in actively breaking crests suggests peak values of order 0.1-0.5. But, peak values of void fraction in the dense plume

model are not appropriate; instead we need a weighted average of the void fraction, where the weighting reflects the different contributions of life stages of the whitecaps to the bubble-mediated gas transfer. In the future, we should base a model on an evolving bubble size distribution and void fraction. Models [*Liang et al.,* 2013] and new observations may enable a better description of bubble-mediated transfer including the suffocation phenomenon.

Using the "independent bubble model" k_w predictions were closest to the N00 parameterization [*Nightingale et al.,* 2000]. However, as explained in section 3.5 we should be cautious when calibrating or validating the hybrid model with k_w data obtained with the DT method because the fraction of bubble-mediated gas transfer is dependent on solubility of the gas. Figure 6 shows the fraction k_b/k_o as a function of wind speed for three gases of different solubility (^{3}He, CO_2 and DMS) at t of 20 °C and s of 35 as predicted by the hybrid model with the W data used here. The fraction increased with increasing wind speed and for $U_{10} \approx 15$ m/s, k_b/k_o is generally higher for ^{3}He than for CO_2. This illustrates that extrapolating DT results of gas transfer velocity for highly soluble gases such as ^{3}He to less soluble gases such as CO_2 could introduce errors, especially for stronger winds. Using the gas transfer velocity models with the *in situ W* data, the terms $k_{b,mod,660}^{DT}$ and $k_{b,mod,660}$ were calculated and their differences plotted against U_{10} in Figure 7. It shows how the differences increased with increasing wind. For the "independent bubble model" the difference is positive and the largest. For the "dense plume model" the difference decreases with increasing void fraction, is near zero for v between 0.2 and 0.3, and negative for larger void fractions. So for low void fractions *Asher and Wanninkhof* [1998]'s suggestion that the dual-tracer method will generally overestimate the transfer velocity of carbon dioxide was confirmed. But if high void fraction bubble plumes dominate, we found that the dual-tracer method may underestimate the transfer velocity of carbon dioxide in agreement with *Woolf* [2007].

The hybrid model presented in this paper could be easily added into the open-source tool boxes of the FluxEngine [*Shutler et al.,* 2015] and that of *Johnson* [2010], to enable users to calculate local, regional and global gas transfer velocities. Through the numerical scheme of *Johnson* [2010] for calculating air-side gas transfer velocity and Schmidt number, the hybrid model could then be evaluated for any gas (section 3.4). Through the FluxEngine the global and regional implications of the model could be evaluated for CO_2. The FluxEngine would also allow the CO_2 gas fluxes to be studied (equations (1) and (13)) and the impact of alternative k_o parameterisations (e.g. the radar altimeter backscatter parameterisation of *Goddijn-Murphy et al.* [2012; 2013]) to be investigated.

6. Conclusion

Data from eddy covariance measurements of DMS and dual tracer experiments give two very distinct views of the behaviour of gas transfer velocity, especially in strong winds. These two sets of data cannot be reconciled by "traditional models" of a quadratic or cubic dependence on wind speed shared by all poorly soluble gases. We show that the data can be reconciled by a semi-empirical model that is based on a distinction between direct and bubble-mediated gas transfer. We use two models of water-side bubble-mediated gas transfer: "the independent bubble model" for which the gas in the bubbles exchanges gas with the surrounding water independently from each other (dissolved gas content of that water is maintained at the mixed-layer average throughout), and the "dense plume model" for which the gas content of the interstitial water is expected to change during the lifetime of the bubble plume. This enables us to assess the effects of the bubble plume's void fraction on bubble-mediated gas transfer and to assess the consequences of bubble-mediated gas transfer for the dual tracer method of measuring gas transfer velocity. Bubble-mediated transfer might be ignored in light to moderate winds but cannot be ignored in stronger winds. The model of air-sea gas

transfer at the ocean surface as a function of wind speed and in the presence of breaking waves can be easily applied to any gas on local, regional and global scales, as long as the gas is chemically unreactive and the fraction of whitecap coverage is known.

ACKNOWLEDGEMENTS

This research is a contribution of the National Centre for Earth Observation, a NERC Collaborative Centre and was supported by the European Space Agency (ESA) Support to Science Element (STSE) project OceanFlux Greenhouse Gases Evolution (contract number: 4000112091/14/I-LG). A. Callaghan acknowledges current financial support from NSF Grant OCE-1434866. Both Jamie Shutler and Phil Nightingale acknowledge funding support from NERC grant NE/K002058/1. The *in situ W* data used here were collected during the MAP (Marine Aerosol Production) project which was an international collaborative effort headed by Prof. Colin O'Dowd (School of Physics and Centre for Climate and Air Pollution Studies, National University of Ireland, Galway, Ireland) and Prof. Gerrit de Leeuw (Climate Change Unit, Finnish Meteorological Institute, Helsinki, Finland and TNO Built Environment and Geosciences, Utrecht, Netherlands) focused on quantifying the production of primary and secondary marine aerosol formation from natural sources. The sea surface images were collected by Leo Cohen (TNO Defence and Security, Hague, Netherlands) and Gerrit de Leeuw on board the R/V Celtic Explorer. The MAP data are available from A. Callaghan upon request (callaghan.adrian@gmail.com).

REFERENCES

Anguelova, M. D. and P. Huq (2012), Characteristics of bubble clouds at various wind speeds, *J. Geoph. Res., 117*, C3, doi: 10.1029/2011JC007442.

Anguelova, M. D. and F. Webster (2006), Whitecap coverage from satellite measurements: A first step toward modelling the variablity of oceanic whitecaps, *J. Geoph. Res., 111*, C3,1-23, doi: 10.1029/2005JC003158.

Asher, W., Edson, J., McGillis, W., Wanninkhof, R., Ho, D. T., Lichtendorf, T. (2002), Fractional area whitecap coverage and air-sea gas transfer velocities measured during GasEx-98., in *Gas transfer at Water Surfaces, Geophys. Monogr., no 127*, edited by M. A. Donelan, W. M. Drennan, E. S. Saltzman, and R. Wanninkhof, pp. 199-203, Amer. Geophys. Union, Washington, DC.

Asher, W. E., L. M. Karle, B. J. Higgins, P. J. Farley, E. C. Monahan, and I. S. Liefer (1996), The influence of bubble plumes on air-seawater gas transfer velocities, *J. Geophys. Res., 101*, 12,027-12,041.

Asher, W. E. and R. Wanninkhof (1998), The effect of bubble-mediated gas transfer on purposeful dual-gaseous tracer experiments., *J. Geophys. Res., 103*, C5, doi: 10.1029/98JC00245.

Bell, T. G., W. J. De Bruyn, C. A. Marandino, S. D. Miller, C. S. Law, M. J. Smith, and E. S. Saltzman (2015), Dimethylsulfide gas transfer coefficients from algal blooms in the Southern Ocean, *Atmos. Chem. Phys, 15*, 1783-1794, doi: 10.5194/acp-15-1783-2015.

Blenkinsopp, C. E. and J. R. Chaplin (2007), Void fraction measurements in breaking waves, *Proc. R. Soc. A., 463*, 3151-3170, doi: 10.1098/rspa.2007.1901.

Bowyer, P. A. (2001), Video measurements of near-surface bubble spectra, *J. Geophys. Res., 106*, 14,179-14,190.

Callaghan, A. H. (2013), An improved whitecap timescale for sea spray aerosol production flux modeling using the discrete whitecap method, *J. Geophys. Res. Atmos., 118*, 17, 9997-10,010, doi: 10.1002/jgrd.50768.

Callaghan, A. H., G. B. Deane, M. D. Stokes, and B. Ward (2012), Observed variation in the decay time of oceanic whitecap foam, *J. Geophys. Res., 117*, C9, doi: 10.1029/2012JC008147.

Callaghan, A. H., G. B. Deane, and M. D. Stokes (2013), Two regimes of laboratory whitecap foam decay: Bubble-plume controlled and surfactant stabilized, *J. Phys. Oceanogr., 43*, 1114-1126, doi: 10.1175/JPO-D-12-0148.1.

Callaghan, A. H., M. D. Stokes, and G. B. Deane (2014), The effect of water temperature on air entrainment, bubble plumes, and surface foam in a laboratory breaking-wave analog, *J. Geophys. Res., 119*, 11, doi: 10.1002/2014JC010351.

Callaghan, A. H., G. B. Deane, and M. D. Stokes (2008a), Observed physical and environmental causes of scatter in whitecap coverage values in a fetch-limited coastal zone, *J. Geophys. R., 113*, C5, doi: 10.1029/2007JC004453.

Callaghan, A., G. de Leeuw, L. Cohen, and C. D. O'Dowd (2008b), Relationship of oceanic whitecap coverage to wind speed and wind history, *Geophys. Res. Lett., 35*, 23, doi: 10.1029/2008GL036165.

Callaghan, A. and M. White (2009), Automated processing of sea surface images for the determination of whitecap coverage*, J. Atmos. Ocean. Tech., 26*, 384-394, doi: 10.1175/2008JTECHO634.1.

Cipriano, R. J. and D. C. Blanchard (1981), Bubble and aerosol spectra produced by a laboratory "breaking wave", *J. Geophys. Res.*, 8085-8092.

de Leeuw, G., E. L. Andreas, M. D. Anguelova, C. W. Fairall, E. R. Lewis, C. O'Dowd, M. Schulz, and S. E. Schwartz (2011), Production flux of sea spray aerosol*, Rev. Geophys., 49*, 2, doi: 10.1029/2010RG000349.

de Leeuw, G. and L. Cohen (2002), Bubble size distributions on the north atlantic and north sea, , in *Gas transfer at Water Surfaces, Geophys. Monogr., no 127*, edited by M. A. Donelan, W. M. Drennan, E. S. Saltzman, and R. Wanninkhof, pp. 271-277, Amer. Geophys. Union, Washington, DC.

Deane, G. B. and M. D. Stokes (2002), Scale dependence of bubble creation mechanisms in breaking waves*, Nature, 418*, 839-844, doi: 10.1038/nature00967.

Donelan, M. A. and R. Wanninkhof (2002), Gas transfer at water surfaces - concepts and issues, in *Gas Transfer at Water Surfaces, Geophys. Monogr., no 127*, edited by M. A. Donelan, W. M. Drennan, E. S. Saltzman, and R. Wanninkhof, pp. 1-10, Amer. Geophys. Union, Washington, DC.

Fairall, C. W., E. F. Bradley, J. E. Hare, A. A. Grachev, and J. B. Edson (2003), Bulk Parameterization of Air–Sea Fluxes: Updates and Verification for the COARE Algorithm*, J. Clim., 16*, 571-591.

Fairall, C. W., M. X. Yang, L. Bariteau, J. B. Edson, D. Helmig, W. R. McGillis, S. Perzoa, J. E. Hare, B. J. Huebert, and B. W. Blomquist (2011), Implementation of the Coupled Ocean-Atmosphere Response Experiment flux algorithm with CO_2, DMS and O_3, *J. Geophys. Res., 116*, C4, doi: 10.1029/2010JC006884.

Fangohr, S. and D. K. Woolf (2007), Application of new parameterization of gas transfer velocity and their impact on regional and global marine CO_2 budgets, *J. Mar. Syst., 66*, 195-203.

Garbe, C. S. et al. (2014), Transfer across the air-sea interface, in *Ocean-Atmosphere Interactions of Gases and Particles*, edited by P. S. Liss and M. T. Johnson, pp. 55-112, Springer, Berlin Heidelberg, doi: 10.1007/978-3-642-25643-1.

Goddijn-Murphy, L. M., D. K. Woolf, and C. A. Marandino (2012), Space-based retrievals of air-sea gas transfer velocities using altimeters: Calibration for dimethyl sulfide, *J. Geophys. Res., 117*, C8, doi: 10.1029/2011JC007535.

Goddijn-Murphy, L. M., D. K. Woolf, B. Chapron, and P. Queffeulou (2013), Improvements to estimating the air-sea gas transfer velocity by using dual-frequency, altimeter backscatter, *Rem. Sens. of Env., 139*, doi: 10.1016/j.rse.2013.07.026.

Goddijn-Murphy, L., D. K. Woolf, and A. H. Callaghan (2011), Parameterizations and algorithms for oceanic whitecap coverage, *J. Phys. Oceanogr., 41*, 742-756, doi: 10.1175/2010JPO4533.1.

Ho, D. T., C. S. Law, M. J. Smith, P. Schlosser, M. Harvey, and P. Hill (2007), Reply to comment by X. Zhang on "Measurements of air-sea gas exchange at high wind speeds in the

Southern Ocean: Implications for global parameterizations", *Geophys. Res. Lett., 34*, 23, 10.1029/2007GL030943.

Ho, D. T., C. S. Law, M. J. Smith, P. Schlosser, M. Harvey, and P. Hill (2006), Measurements of air-sea gas exchange at high speed winds in the Southern Ocean: Implications for global parameterizations, *Geophys. Res. Lett., 33,* L16611, doi:10.1029/2006GL026817.

Hoque, A. and S. Aoki (2014), Wave-energy dissipation and wave setup caused by entrained air bubbles in plunging wave breaking, *J. Waterw. Port Coast. Ocean Eng., 140*, doi: 10.1061/(ASCE)WW.1943-5460.0000252.

Huebert B., B. Blomquist, M. Yang, S.D. Archer, P.D. Nightingale, M.J. Yelland, J. Stephens, R.W. Pascal, B.I. Moat (2010), Linearity of DMS transfer coefficient with both friction velocity and wind speed, *Geophys. Res. Lett. 37* DOI: 10.1029/2009gl041203.

Jähne, B., K. O. Münnich, R. Bösinger, A. Dutzi, W. Huber, and P. Libner (1987), On the parameters influencing air-water gas exchange, *J. Geophys. Res., 92*, 1937-1949.

Jeffery, C. D., D. K. Woolf, I. S. Robinson, and C. J. Donlon (2007), 1-D modelling of convective CO2 exchange in the Tropical Atlantic, *Ocean Model., 19*, 182, doi: 10.1016/j.ocemod.2007.07.003.

Jeffery, C. D., I. S. Robinson, and D. K. Woolf (2010), Tuning a physically-based model of the air-sea gas transfer velocity, *Ocean Model., 31*, 28-35, doi: 10.1016/j.ocemod.2009.09.001.

Johnson, M. T. (2010), A numerical scheme to calculate temperature and salinity dependent air-water transfer velocities for any gas, *Ocean Sci., 6*, 913-932, doi: 10.5194/os-6-913-2010.

Keeling, R. F. (1993), On the role of large bubbles in air-sea gas exchange and supersaturation in the ocean., *J. Mar. Res., 51*, 237-271.

Kiger, K. T. and J. H. Duncan (2012), Air-entrainment mechanisms in plunging jets and breaking waves, *Annu. Rev. Fluid Mech., 44*, 563-596, doi: 10.1146/annurev-fluid-122109-160724.

Lamarre, E. and W. K. Melville (1991), Air entrainment and dissipation in breaking waves, *Nature, 351*.

Leifer, I. and G. d. Leeuw (2006), Bubbles generated from wind-steepened breaking waves: 1. Bubble plume bubbles, *J. Geophys. Res., 111*(C06020), doi: 10.1029/2004JC002673.

Liang, J. -., C. Deutsch, J. C. McWilliams, B. Baschek, P. P. Sullivan, and D. Chiba (2013), Parameterizing bubble-mediated air-sea gas exchange and its effect on ocean ventilation , *Global Biochem. Cy., 27*, 894-905, doi: 10.1002/gbc.20080.

Lim, H. J., K. A. Chang, Z. C. Huang, and B. Na (2015), Experimental study on plunging breaking waves in deep water, *J. Geophys. Res., 120*, 3, 2007-2049, doi: 10.1002/2014JC010269.

Liss, P. S. and L. Merlivat (1986), Air-sea gas exchange rates: Introduction and synthesis, in *The Role of Air-Sea Exchange in Geochemical Cycling*, edited by P. Buat-Menard, pp. 113-127, D Reidel, Dordrect.

McGillis, W. R., J. W. H. Dacey, N. M. Frew, E. J. Bock, and R. K. Nelson (2000), Water-air flux of dimethylsulfide, *J. Geophys. Res., 105*, C1, 1187-1193.

McGillis, W. R., J. B. Edson, J. D. Ware, J. W. H. Dacey, J. E. Hare, C. W. Fairall, and R. Wanninkhof (2001), Carbon dioxide flux techniques performed during GasEx 98, *Mar. Chem., 75*, 267-280.

Monahan, E. C. (1971), Oceanic whitecaps*, J. Phys. Oceanogr., 172*, 139-144.

Monahan, E. C. and M. Lu (1990), Acoustically relevant bubble assemblages and their dependence on metereological parameters*, J. Oceanic Eng., 15*, 340-349.

Monahan, E. C., C. W. Fairall, K. L. Davidson, and P. Jones Boyle (1983), Observed inter-relations between 10m winds, ocean whitecaps and marine aerosols*, Quart. J. R. Met. Soc., 109*, 379-392.

Nightingale, P. D. (2009), Air-sea gas exchange, in *Surface Ocean—Lower Atmosphere Processes*, vol. 187, edited by C. Le Quéré and E. S. Saltzman, pp. 69-97, AGU, Washington, D. C.

Nightingale, P. D., G. Malin, C. S. Law, A. J. Watson, and P. S. Liss (2000), In situ evaluation of air-sea gas exchange parameterizations using novel conservative and volatile tracers*, Global Biochem. Cy., 14*, 373-387.

Prytherch, J., M. J. Yelland, R. W. Pascal, B. I. Moat, I. Skjelvan, and M. A. Srokosz (2010), The open ocean gas transfer velocity derived from long-term direct measurements of the CO_2 flux*, Geophys. Res. Lett., 37*, L23607, doi: 10.1029/2010GL045597.

Sharkov, E. A. (2007)*, Breaking Ocean Waves: Geometry, Structure and Remote Sensing,* Springer, Chichester, U. K.

Shutler, J.D, Land, P. E., Piolle, J.-F., Woolf, D. K., Goddijn-Murphy, L, Paul, F.,Girard-Ardhuin, F., Chapron, B., and Donlon, C. J. (2015), FluxEngine: A flexible processing system for calculating atmosphere-ocean carbon dioxide gas fluxes and climatologies. *J. Atmos. Ocean. Tech.*, *in press*, doi: 10.1175/JTECH-D-14-00204.1.

Stokes, D., G. Deane, S. Vagle, and D. Farmer (2002), Measurements of large bubbles in open-ocean whitecaps, in *Gas transfer at Water Surfaces, Geophys. Monogr., no 127*, edited by Donelan, M.A. Drennan, W.M. Saltzman, E.S., Wanninkhof, R., Amer. Geophys. Union, Washington, D. C..

Sweeney, C., E. Gloor, A. R. Jacobson, R. M. Key, G. McKinley, J. L. Sarmiento, and R. Wanninkhof (2007), Constraining global air-sea gas exchange for CO_2 with recent bomb ^{14}C measurements*, Global Biogeochem., 21*, 2, doi: 10.1029/2006GB002784.

Takahashi, T. et al. (2009), Climatological mean and decadal change in surface ocean pCO2, and net sea–air CO2 flux over the global oceans*, Deep-Sea Res. II, 56*, 554-577, doi: 10.1016/j.dsr2.2008.12.009.

Wanninkhof, R. (2014), Relationship between wind speed and gas exchange over the ocean revisited*, Limnol. Oceanogr. Methods, 12*, 351-362, doi: 10.4319/lom.2014.12.351.

Wanninkhof, R. (1992), Relationship between wind speed and gas excahnge over the ocean*, J. Geophys. R., 97*, 7373-7382.

Wanninkhof, R., W. E. Asher, D. T. Ho, C. Sweeney, and W. R. McGillis (2009), Advantages in Quantifying AirSea Gas Exchange and Environmental Forcing*, Annu. Rev. Mar. Sci., 1*, 213-244, doi: 10.1146/annurev.marine.010908.163742.

Wanninkhof, R. and W. R. McGillis (1999), A cubic relationship between air-sea CO_2 exchange and wind speed, *Geophys. Res. Lett., 26*, 13, 1889-1892.

Watson, A. J., R. C. Upstill-Goddard, and P. S. Liss (1991), Air–sea gas exchange in rough and stormy seas measured by a dual-tracer technique, *Nature, 349*, 145-147, doi: 10.1038/349145a0.

Woolf, D. K. (1993), Bubbles and the air-sea transfer velocity of gases, *Atmos. Ocean, 31*, 517-540.

Woolf, D. K. and S. A. Thorpe (1991), Bubbles and the air-sea exchange of gases in near-saturation conditions, *J. of M. Res., 49*, 435-466.

Woolf, D. (1997), Bubbles and their role in air-sea gas exchange, in *The Sea Surface and Global Change*, edited by P. S. Liss and R. A. Duce, pp. 173-205, Cambridge University Press, Cambridge.

Woolf, D. K. (2005), Parametrization of gas transfer velocities and sea-state-dependent wave breaking, *Tellus, 57-B*, 87-94.

Woolf, D. K. et al. (2007), Modelling of bubble-mediated gas transfer: Fundamental principles and laboratory test, *J. Mar. Syst., 66*, 71-91, doi: 10.1016/j.jmarsys.2006.02.011.

Yang, M., B. W. Blomquist, and P. D. Nightingale (2014), Air-sea exchange of methanol and acetone during HuWinGS: Estimation of air phase, water phase gas transfer velocities, *J. Geophys. Res., 119*, 10, 7308-7323, doi: 10.1002/2014JC010227.

Yang, M., P. D. Nightingale, R. Beaea, P. S. Liss, B. Blomquist, and C. Fairall (2013), Atmospheric deposition of methanol over the Atlantic Ocean*, PNAS, 110*, 50, 20034-20039, doi: 10.1073/pnas.1317840110.

Table captions

Table 1. The main assumptions made in the bubble model and their estimated magnitudes

Table 2. "Wind speed only" k_w parameterizations. Gases: CO_2 (carbon dioxide), N_2O (nitrous oxide), ^3He (3-Helium), SF_6 (sulphur hexafluoride), and DMS (dimethyl sulphide); Methods: eddy covariance (EC), dual tracer (DT), ^{14}C (curve fit such that when averaged over global wind speeds it is in agreement with the global mean k_w determined from the oceanic uptake of bomb derived radiocarbon).

Table 3. Bubble-mediated gas transfer of CO_2 at 20 °C and salinity of 35 of 1% W using the "independent plume model" (equation (8)), and "dense plume model" and a range of void fractions (equation (9)).

Figure captions

Figure 1. Range of U_{10}- $k_{w,660}$ parameterizations, see Table 2 for details.

Figure 2. Bubble-mediated gas transfer of CO_2 at 20 °C and salinity of 35 for W = 1% using the "dense plume model" and a range of void fractions (equation (9)).

Figure 3 (a,b). Panel a shows the canonical bubble size distribution reported by Deane and Stokes [2002] for laboratory breaking waves with the Hinze Scale set to a bubble radius of 1.5 mm (solid line), and this distribution scaled by bubble volume (dashed line). The power law bubble distribution at bubble radii less than and greater than the Hinze scale has slopes of -3/2 and -10/3 respectively, as indicated in panel a. These slopes change to 3/2 and -1/3, respectively, when the distribution is scaled by bubble volume. The peak of the bubble volume distribution indicates that bubbles at the Hinze scale have the largest single contribution to the initial volume of air entrained during breaking. Panel b shows a probability density function of air volume as a function of bubble radius, indicating that supra-mm bubbles are expected to account for the majority of the air volume in an actively breaking crest.

Figure 4. The difference between equation (15) and equation (8) (or equation (9)) if "independent bubble plume" (or "dense bubble plume" with "v" indicating the void fraction) is used for CO_2 in seawater of 20 °C; for 1 W%. This figure shows the modelled propagation of the error due to the different contributions of bubble-mediated gas transfer of the two gases used in the dual tracer method.

Figure 5 (top) As Figure 1 but with Hybrid model (equation (6)) using the "independent bubble model" (equation (8)) and the in-situ W data to calculate breaking term; with the

black dots indicating the model results and the circles the model results binned in 1 m/s bins with error bars the standard errors. (bottom) Hybrid model results of $k_{w,660}$ using equations (6), (8) and (9) and the in-situ W data to calculate breaking term; with the black dots indicating the "independent bubble model" and the open circles the "dense plume model" with void fraction of 0.5. Not shown: all "dense plume model" estimations of $k_{w,660}$ are below those of the "independent bubble model" and $k_{w,660}$ values for v greater / smaller than 0.5 are over / under those for v of 0.5. All equations were calculated for CO_2 in seaweter of °C.

Figure 6. Fractions of k_b/k_o according to equations (11) and (12) for gases ^3He, CO_2, and DMS at t = 20 °C and s = 35 (^3He, α = 0.008, Sc = 144; CO_2, α = 0.727, Sc = 660; DMS, α = 12.73, Sc = 918 [*Wanninkhof et al.,* 2009]) *and using the in situ W data to calculate k_b with (a) equation (8), the "independent bubble model"(8), and (b) equation (9), the " dense plume model" with v of 0.2.*

The difference between equation (15) and equation (8) (or equation (9)) if "independent bubble plume" (or "dense bubble plume" with "v" indicating the void fraction) is used for CO_2 in seawater of 20 °C. This is the same difference as shown in Figure 4 but multiplied by MAP whitecap fraction, W, and using MAP data for t (~13 °C) and U_{10}.

Tables

Table 1. The main assumptions made in the bubble model and their estimated magnitudes

Assumption	*Reasonably soluble*	*Very poorly soluble*
Supersaturation term, δ, small [*Woolf et al,* 2007]	$\delta \approx 0$	$\delta \approx 3\%$ (for 0.6m depth)
Large bubbles [*Deane and Stokes,* 2002; *Woolf et al,* 2007]	Small bubbles less important	Small bubbles more important (δ)
Clean bubble surface [Woolf, *1993*]	Dirty bubble surface: $k_{b,ind} = 2.6W\%$ instead of $8.5W\%$	Dirty bubble surface: $k_{b,ind} = 3.7W\%$ instead of $14.1W\%$
Shallow flux [*Woolf et al*., *2007*]	Deep flux: more dirty bubbles.	Deep flux: more dirty and more small bubbles; ρ increases with depth.

Table 2. "Wind speed only" k_w parameterizations. Gases: CO_2 (carbon dioxide), N_2O (nitrous oxide), ^3He (3-Helium), SF_6 (sulphur hexafluoride), and DMS (dimethyl sulphide); Methods: eddy covariance (EC), dual tracer (DT), ^{14}C (curve fit such that when averaged over global wind speeds it is in agreement with the global mean k_w determined from the oceanic uptake of bomb derived radiocarbon).

Source		Gases used	method
[*Liss and Merlivat,* 1986]	LM86	U_{10} <= 13 m/s, SF_6	Lake /
		U_{10} > 13 m/s, CO_2 and N_2O	Laboratory
[*Wanninkhof,* 1992]	W92	CO_2	^{14}C
[*Wanninkhof and McGillis,* 1999]	WM99	CO_2	^{14}C
[*Nightingale et al.,* 2000]	N00	^3He and SF_6	DT
[*McGillis et al.,* 2001]	M01	CO_2	EC
[*Ho et al.,* 2006]	H06	^3He and SF_6	DT
[*Wanninkhof et al.,* 2009]	W09	CO_2	^{14}C
[*Prytherch et al.,* 2010]	P10	CO_2	EC
[*Goddijn-Murphy et al.,* 2012]	G12	DMS	EC

Table 3. Bubble-mediated gas transfer of CO_2 at 20 °C and salinity of 35 of 1% W using the "independent plume model" (equation (8)), and "dense plume model" and a range of void fractions (equation (9)).

model	$k_{b,mod,660}$ (cm/h)
independent	8.65
v (dense plume)	
0.1	8.25
0.2	7.80
0.3	7.29
0.4	6.72
0.5	6.08
0.6	5.32
0.7	4.42
0.8	3.33
0.9	1.94
1	0

Figures

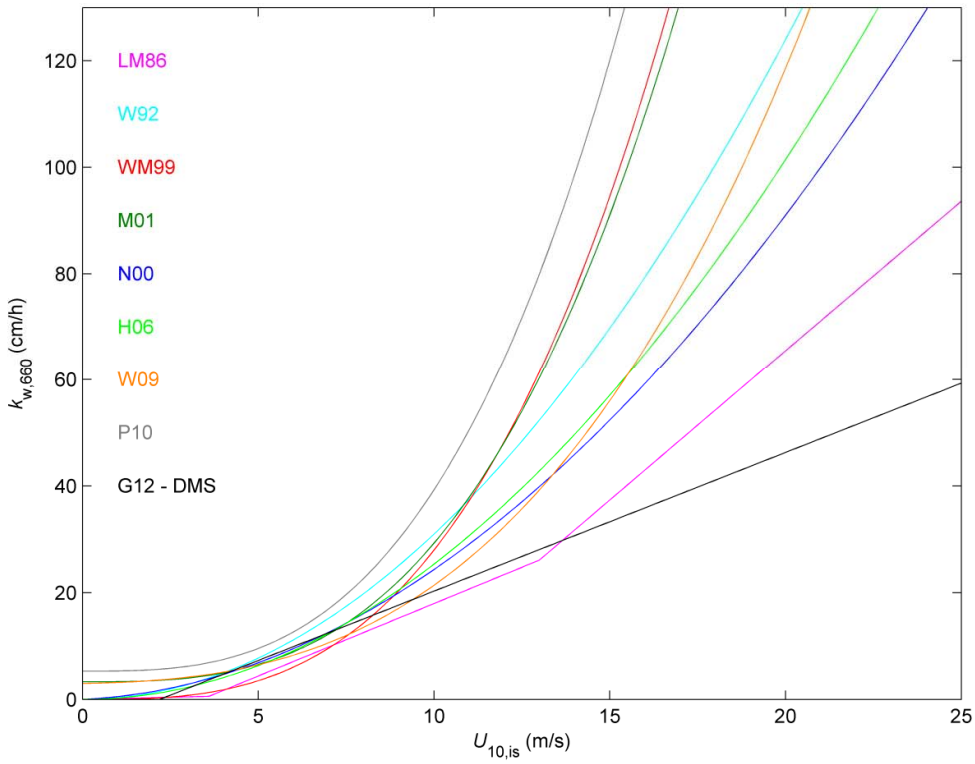

Figure 1. Range of U_{10}- $k_{w,660}$ parameterizations, see Table 2 for details.

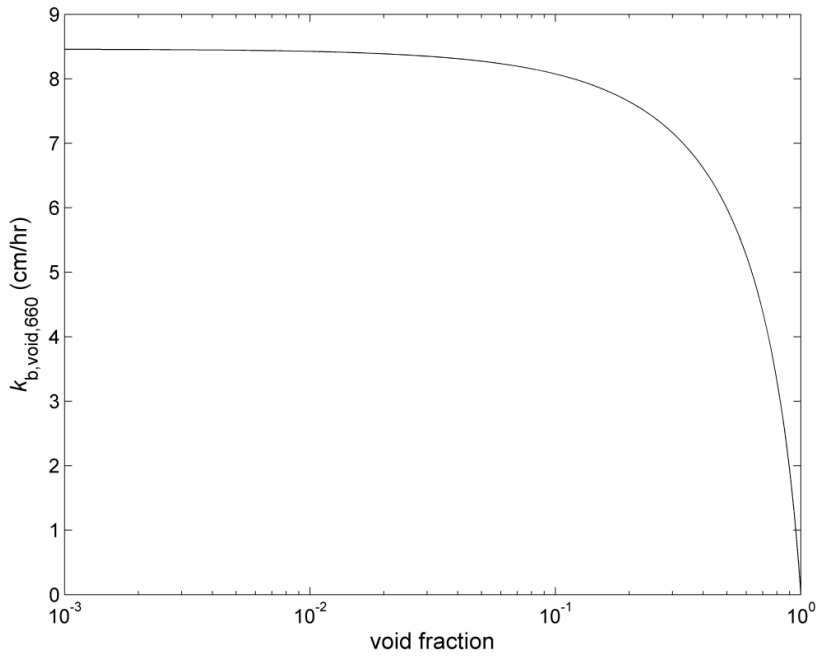

Figure 2. Bubble-mediated gas transfer of CO_2 at 20 °C and salinity of 35 for W = 1% using the "dense plume model" and a range of void fractions (equation (9)).

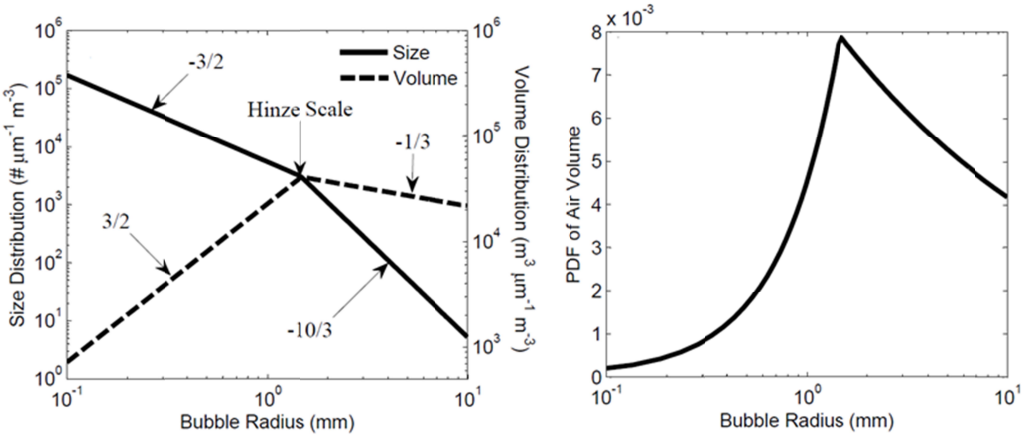

Figure 3 (a,b). Panel a shows the canonical bubble size distribution reported by Deane and Stokes [2002] for laboratory breaking waves with the Hinze Scale set to a bubble radius of 1.5 mm (solid line), and this distribution scaled by bubble volume (dashed line). The power law bubble distribution at bubble radii less than and greater than the Hinze scale has slopes of -3/2 and -10/3 respectively, as indicated in panel a. These slopes change to 3/2 and -1/3, respectively, when the distribution is scaled by bubble volume. The peak of the bubble volume distribution indicates that bubbles at the Hinze scale have the largest single contribution to the initial volume of air entrained during breaking. Panel b shows a probability density function of air volume as a function of bubble radius, indicating that supra-mm bubbles are expected to account for the majority of the air volume in an actively breaking crest.

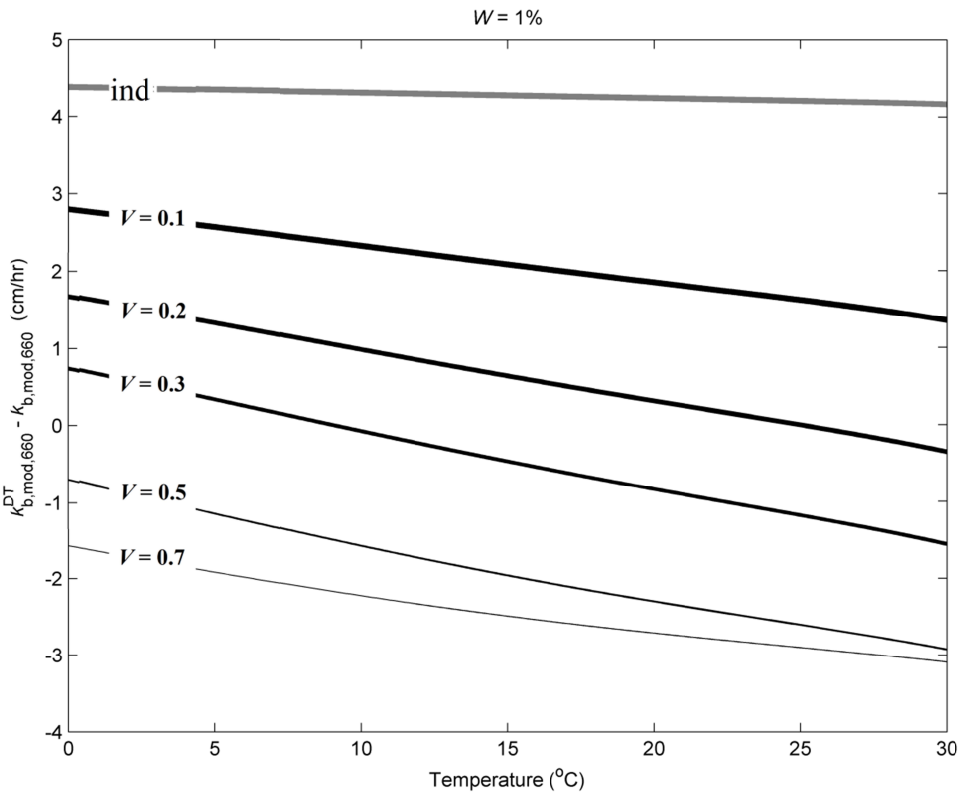

Figure 4. The difference in $k_{b,660}$ for W = 1% according to the bubble models (equations (8)-(9)) if dual tracer technique is used (equation (15)) and if modelled directly, as a function of temperature; for the "independent bubble plume" (ind) and the "dense plume model" and a range of void fractions (v).The difference between equation (15) and equation (8) (or equation (9)) if "independent bubble plume" (or "dense bubble plume" with "v" indicating the void fraction) is used for CO_2 in seawater of 20 °C; for 1 W%. This figure shows the modelled propagation of the error due to the different contributions of bubble-mediated gas transfer of the two gases used in the dual tracer method.

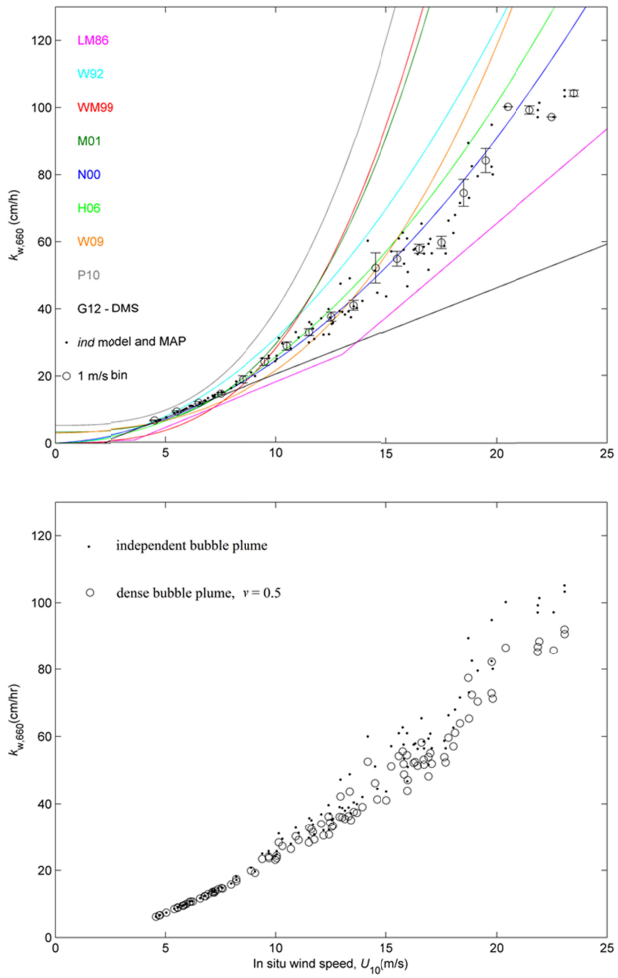

Figure 5 (top) As Figure 1 but with Hybrid model (equation (6)) using the "independent bubble model" (equation (8)) and the in-situ W data to calculate breaking term; with the black dots indicating the model results and the circles the model results binned in 1 m/s bins with error bars the standard errors;. (bottom) Hybrid model results of $k_{w,660}$ using equations (6), (8) and (9) and the in-situ W data to calculate breaking term; with the black dots indicating the "independent bubble model" and the open circles the "dense plume model" with void fraction of 0.5. Not shown: all "dense plume model" estimations of $k_{w,660}$ are below those of the "independent bubble model" and $k_{w,660}$ values for v greater / smaller than 0.5 are over / under those for v of 0.5. All equations were calculated for CO_2 in seawater of 20 °C.

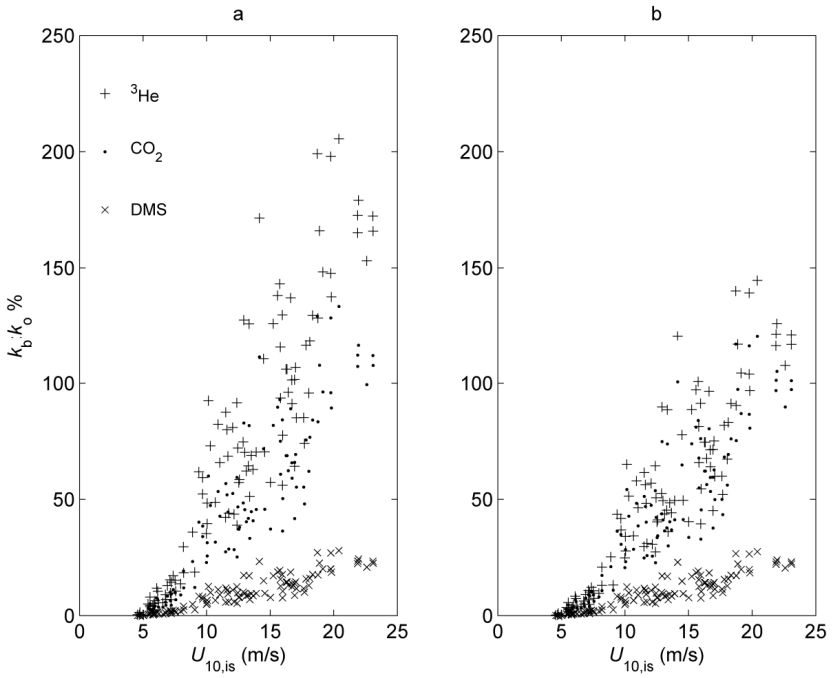

Figure 6. Fractions of k_b/k_o according to equations (11) and (12) for gases ^{3}He, CO_2, and DMS at t = 20 °C and s = 35 (^{3}He, α = 0.008, Sc = 144; CO_2, α = 0.727, Sc = 660; DMS, α = 12.73, Sc = 918 [*Wanninkhof et al.,* 2009]) *and using the in situ W data to calculate k_b with (a) equation (8), the "independent bubble model"(8), and (b) equation (9), the " dense plume model" with v of 0.2.*

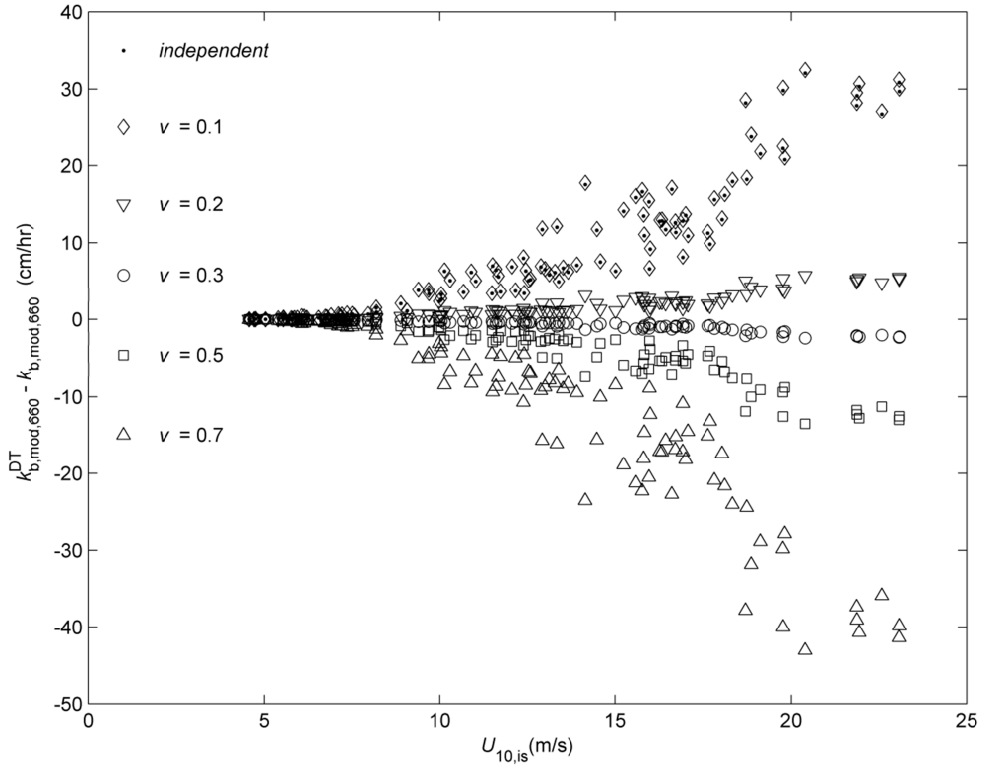

Figure 7. The difference between equation (15) and equation (8) (or equation (9)) if "independent bubble plume" (or "dense bubble plume" with "v" indicating the void fraction) is used for CO_2 in seawater of 20 °C. This is the same difference as shown in Figure 4 but multiplied by MAP whitecap fraction, W, and using MAP data for t (~13 °C) and U_{10}.